Ocean Systems Engineering, *Vol. 5, No. 2 (2015) 109-123*
DOI: http://dx.doi.org/10.12989/ose.2015.5.2.109

Numerical simulation of the coupled dynamic response of a submerged floating tunnel with mooring lines in regular waves

Cristian Cifuentes[1], Seungjun Kim[1], M.H. Kim[*1] and W.S. Park[2]

[1]*Ocean Engineering Program, Department of Civil Engineering, Texas A&M University College Station, Texas, USA*
[2]*KIOST, Korea*

(Received May 28, 2015, Revised June 5, 2015, Accepted June 8, 2015)

Abstract. In the present study, the coupled dynamic response of a Submerged Floating Tunnel (SFT) and mooring lines under regular waves is solved by using two independent numerical simulation methods, OrcaFlex and CHARM3D, in time domain. Variations of Buoyancy to Weight Ratio (BWR), wave steepness/period, and water/submergence depth are considered as design and environmental parameters in the study. Two different mooring-line configurations, vertical and inclined, are studied to find an optimum design in terms of limiting tunnel motions and minimizing mooring-line tension. The numerical results are successfully validated by direct comparison against published experimental data. The results show that tunnel motions and tether tensions grow with wave height and period and decrease with submergence depth. The inclined mooring system is more effective in restricting tunnel motions compared to the vertical mooring system. Overall, the present study demonstrates the feasibility of this type of structure as an alternative to traditional bridges or under-seabed tunnels.

Keywords: SFT (Submerged Floating Tunnel); tethers; coupled dynamics; FEM/BEM (Finite/Boundary Element Method); drag coefficient; BWR (Buoyancy to Weight Ratio); vertical/inclined mooring; line tensions

1. Introduction

In countries such as Norway and Italy where there are many narrow fjords and straits, SFT(Submerged Floating Tunnel) is considered as an alternative for land connections. SFT is a simple structure that is installed underwater at a given depth, kept in place by the combination of positive buoyancy and tethers anchored to the sea bed (Di Pilato *et al.* 2008). The SFT concept was well understood at the end of the 19th century and the interest for this type of structure was revived in the 1960's with some minor research effort in Norway and Italy (Østlid 2010).

Subsequently, further studies were made to better understand the dynamic response of a SFT (Hong and Ge 2010). Since then, although no such a structure has ever been built, the interest for the concept grows in the engineering community. A complete guide for the design and characteristics of a SFT can be found in the work by Jakobsen (2010) summarizing several feasibility studies carried out in Norway.

*Corresponding author, Professor, E-mail: m-kim3@tamu.edu

http://www.techno-press.org/?journal=ose&subpage=7 ISSN: 2093-6702 (Print), 2093-677X (Online)

In order to design and install a SFT structure, analyses under multiple load scenarios are necessary. For real design and construction, a rational global performance analysis technique including mooring lines should be developed. By performing a global performance analysis, engineers can simulate the static/dynamic behavior of SFT under various environmental loading conditions and then observe important features of the system, such as motions, internal forces and anchor reactions, and structural stresses of the tunnel and tethers. In addition, structural safety, structural stability, fatigue damage and operational life can also be estimated.

Some of the critical loads and hazards include (a) hydrostatic pressure and self-weight, (b) environmental loads including waves, current, earthquakes and internal waves, (c) loads due to internal traffic and ballast, and (d) accidental loads such as internal explosions, collisions, and mooring system failure (Lu *et al*. 2011). In addition, fatigue of tethers due to Vortex Induced Vibration (VIV) is also of interest for design and operational stages (Hong and Ge 2010).

Several researchers have performed analyses and experiments for SFT under mainly regular wave loading. Examples include global performance analysis focused on tether tension and tunnel displacements carried out by Kunisu *et al*. (1994) which revealed direct proportionality between wave height and mooring line tension. The direct relations between surge-heave amplitude and BWR was presented by Hong and Ge (2010) based on a series of experiments. The experimental findings include (i) as pretension increases with bigger BWR, the translational displacements are increased, (ii) the submergence depth has a significant impact on the reduction of dynamic responses due to the reduction of pressure fluctuations over the submerged tunnel (Oh *et al*. 2013).

Wave directionality and wave-current interactions are also important factors to consider in the design of a SFT. Many numerical tools, such as computational fluid dynamics (CFD), fluid structure interaction (FSI), finite element method (FEM), and stochastics dynamics methods need to be developed for the detailed study. Analytical solutions have also been developed to estimate forces over submerged cylinders exposed to waves (Romolo *et al*. 2008). Each method can provide invaluable information at some steps into the design process. Nonlinearities such as drag loads and large displacements can be obtained in time domain using those numerical procedures (Kunisu 2010). The combined effects of hydrodynamic and seismic loads was reported in Pilato *et al*. (2008). For wave induced dynamic loadings, either Morison model or BEM (Boundary Element Method) can be used (Kunisu 2010).

Other nonlinearities can also be included in time domain analysis. One example is the presence of snap loads over the tethers under slack condition. This situation is undesired since high tensions are induced for a short period of time prompting high stresses over the anchor and connection points to the submerged tunnel. Lu *et al*. (2011, 2013) showed the influence of the inclination angle of tethers over the presence of snap loads.

Based on previous findings, the present work looks into the global performance and coupled dynamic response of the submerged floating tunnel and mooring system by using two different numerical approaches, OrcaFlex (Orcina 2015) and CHARM3D (Kim *et al.* 2005, Bae and Kim 2014, Kang and Kim 2014, Eom *et al.* 2014, Yang 2009). Differences in the numerical models arise in mooring-line treatment i.e., OrcaFlex uses a lumped mass model, while CHARM3D uses FEM approach proposed by Garret (1982). In both cases, the tunnel is excited under regular wave loading where crest lines are in parallel with the axial direction of tunnel as presented in Fig. 1.

Conditions analyzed in this study include a wide range of wave steepness, BWR, water depth, and two mooring configurations. Both numerical results for tether tensions and tunnel displacements are systematically compared with experimental results by Oh *et al*. (2013).

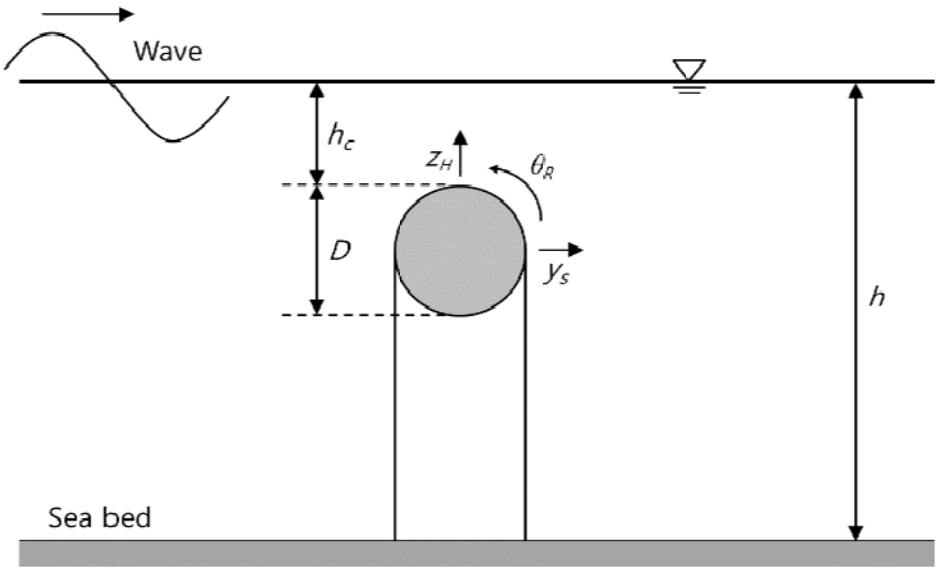

Fig. 1 SFT under vertical mooring configuration

2. Description of numerical models

As previously mentioned, two different computer programs have been applied in this analysis. The first code is OrcaFlex, a commercial software widely used in the offshore industry for the global analysis of moored floating platforms and underwater pipe installation with capabilities to perform fatigue and VIV analysis when coupled to external codes (Orcina 2015). The second tool, the boundary/finite element program CHARM3D (Coupled Hull And Riser Mooring 3D) (Kim *et al.* 2005, Bae and Kim 2014, Kang and Kim 2014, Eom *et al.* 2014, Yang 2009), was also used in this study. The code has been developed by the 3rd author's research lab for the fully coupled dynamic analysis of moored offshore structures with extended capabilities for additional coupling with CFD programs, wind turbines (Bae and Kim 2014), hydro elasticity (Kang and Kim 2014), DP/control and riser design (Eom *et al.* 2014). A brief summary for both codes is presented in the following section.

2.1 Simulations by CHARM3D

The program is able to complete fully coupled dynamic analysis for platform and mooring systems in frequency and time domain including first- and second-order sum- and difference-frequency wave effects. In time domain, several nonlinearities can be applied including drag forces on mooring lines and floaters at their instantaneous positions and nonlinear mooring effects.

For modeling the mooring lines, the rod theory proposed by Garret (1982) is used. A brief summary is given below. The details of the FE (finite element) formulations are, for example,

explained in (Kim *et al.* 2005, Bae and Kim 2014, Kang and Kim 2014, Eom *et al.* 2014, Yang 2009).

The position of the rod centerline determines the behavior of the element. A position vector *r(s,t)* as function of arc length *s* and time *t* defines the coordinate system. The equation of motion is given by a contribution of bending and axial stiffness, distributed load and mass and hydrostatic and hydrodynamic loads.

$$-(EIr'')'' + (\lambda r')' + q = \rho_r \ddot{r}$$

$$r' \cdot r' = \left(1 + \frac{T}{EA_I}\right)^2 \approx 1 + 2\frac{\lambda}{EA_I} \tag{1}$$

In Eq. (1), E=Young's modulus of the rod, I=cross sectional moment of inertia, q= distributed load, ρ_r= rod density, T= axial tension, A_I= cross sectional area, and λ=Lagrangian multiplier. Dots represent derivatives with respect to time while apostrophes represent position derivatives.

The distributed load can be modified to include hydrostatic and hydrodynamic loading as presented in Eq. (2) where w= rod weight by unit length, F^s= hydrostatic force per unit length, and F^d= hydrodynamic force per unit length.

$$q = w + F^s + F^d \tag{2}$$

Further, the hydrostatic load can be represented as Eq. (3), where B= represents buoyancy force per unit length and P= hydrostatic pressure at point r on the rod.

$$F^s = B - (PA_I r')' \tag{3}$$

The last piece on the final equation of motion is the determination of the hydrodynamic force which is calculated based on Morison equation considering relative motion (Haritos and He 1992). The particular form used in this analysis is presented in Eq. (4) where C_A, C_M and C_D are added mass, inertia and drag coefficients, $\dot{r}^n$ and $\ddot{r}^n$ = component of the rod member velocity and acceleration normal to rod centerline, ρ= water density, A_D= area of the unit length rod projected to the plane normal to the rod centerline, V^n and $\dot{V}^n$ = velocity and acceleration of the water normal to the rod centerline due to the incident wave and current.

$$F^d = -C_A \rho A_I \ddot{r}^n + C_M \rho A_I \dot{V}^n + \frac{1}{2} C_D \rho A_D \left|V^n - \dot{r}^n\right| (V^n - \dot{r}^n)$$
$$C_M = C_A + 1 \tag{4}$$

By combining Eqs. (1)-(3) we obtain the final form of the equation of motion for the rod.

$$m\ddot{r} + C_A \rho A_I \ddot{r}^n + (EIr'')'' - (\tilde{\lambda} r')' = \tilde{w} + \tilde{F}^d$$

where

$m = mass\ per\ unit\ length$

$\tilde{\lambda} = \tilde{T} - EI\kappa^2$

$\kappa = local\ curvature$

$\tilde{w} = w + B : wet\ weight\ of\ the\ rod$

$\tilde{T} = T + P : effective\ tension\ in\ the\ rod$

$$\tilde{F}^d = C_M \rho A_I \dot{V}^n + \frac{1}{2} C_D \rho A_D \left| V^n - \dot{r}^n \right| (V^n - \dot{r}^n) \tag{5}$$

After solving for r and λ, the displacements and forces acting over the tunnel can be found. The previous equations are solved following a nonlinear finite element procedure in time domain with second order accuracy.

In this code, fixed values were used for C_D and C_M based on standard values given for cylinders under wave action.

2.2 Simulations by OrcaFlex

In OrcaFlex, a combination of lines and 3 degree of freedom buoys are used to discretize the system. In OrcaFlex, lines are modeled as massless springs connected to each other by nodes. Springs represent axial, torsional and bending properties of the segment using a combination of springs and dampers model, while mass, buoyancy and drag forces are lumped into the nodes (Orcina 2015). The hydrodynamic load over line elements is calculated in a similar manner as presented in Eq. (4) and the final equation of motion includes effects from axial tension, internal and external pressures for the case of pipes, buoyancy, gravity, torsion and bending. In the present case, torsion and internal pressure effects are not included. Three degree of freedom buoys are used to connect the element representing the SFT and the mooring lines. The hydrodynamic contribution of these elements is neglected since they served just as connection nodes, thus its formulation is omitted.

In order to calculate the global response of the system, a local equation of motion must be solved first for each element. The form of this equation of motion is given in Eq. (6). In this case an implicit integration scheme has been selected, using a constant time step and the Generalized α integration scheme. Therefore an iterative solution at the end of each time step is reached. This method allows stable simulations for longer time steps (Orcina 2015).

$$M(p,a) = F(p,v,t) - C(p,v) - K(p) \tag{6}$$

In Eq. (6), *M(p,a)* is the local inertia load, *F(p,v,t)* is the external load over the element, *C(p,v)* is the element damping load and *K(p)* is the element stiffness load. *p,v,a* and *t* are the position, velocity, acceleration and simulation time step respectively. The forcing component *F(p,v,t)* includes $F^d(t)$ in addition to buoyancy and gravity forces. The global equation of motion for the system has the same form as the local one except that it uses global loads and vectors.

In OrcaFlex, C_M is a fixed value while C_D varies during the simulation time according to the normal relative velocity between line element and flow field. This formulation is based on the work by DeCew (2010) and is suitable to describe variation of C_D values for underwater cylinders (Cifuentes and Kim 2015). The expression for C_D is defined up to Re=10e7 capturing the drop in drag coefficient due to the transition to turbulent flow. The formulation is presented in Eq. (7).

$$C_D = \begin{cases} \dfrac{8\pi}{Res}(1-0.87s^{-2}), & 0 < Re < 1 \\ 1.45 + 8.55Re^{-0.9}, & 1 < Re \le 30 \\ 1.1 + 4Re^{-0.5}, & 30 < Re \le 2.33x10^5 \\ -3.41x10^{-6}(Re - 5.78x10^5), & 2.33x10^5 < Re \le 4.92x10^5 \\ 0.401(1 - e^{-Re/5.99x10^5}), & 4.92x10^5 < Re \le 10^7 \\ s = -0.077215655 + ln(8/Re) & \end{cases} \tag{7}$$

By using this method, accurate hydrodynamic loads can be computed for the SFT structure as well as for mooring lines.

Another important point is that in the code CHARM3D, the SFT was modeled using the prototype dimensions, while on OrcaFlex, SFT was modeled using the laboratory conditions in order to detect any scaling effect when checking the results. In both codes, waves are gradually applied by using a ramping function at the early stages of the numerical computation. By using this procedure, the simulation is stable and sudden changes on tension and displacements are avoided.

3. Physical experiments

The numerical analysis is compared with the experimental results presented in the work by Oh *et al.* (2013). In that study, the dynamic response of a single SFT section under wave loading is analyzed. The experiments were carried in a two dimensional wave tank, 53-m long, 1.25-m high and 1-m wide. Several parameters are varied in the experiment to reveal its dynamic characteristics depending on design parameters. Main results from this study are motions of the SFT and forces on mooring components. The configuration for vertical and inclined tethers used in the experiment is given in Figs. 1 and 2.

The SFT is installed with its center at 50 cm over the bottom of the tank. The experiment considers 1:100 scale factor. Mooring lines form a 30 degree angle with respect to a vertical plane in Fig. 2(b). BWR (buoyancy-weight ratio) variation is obtained by adding ballast to the tube. Motion tracking devices follow the displacements of two targets on the body to obtain accurate measurements of motions. Waves were generated for 60 seconds for each test condition as presented in Table 1. Both configurations, vertical and inclined mooring systems, were analyzed under the same wave conditions. More details of the experimental set up are given in Oh *et al.* (2013).

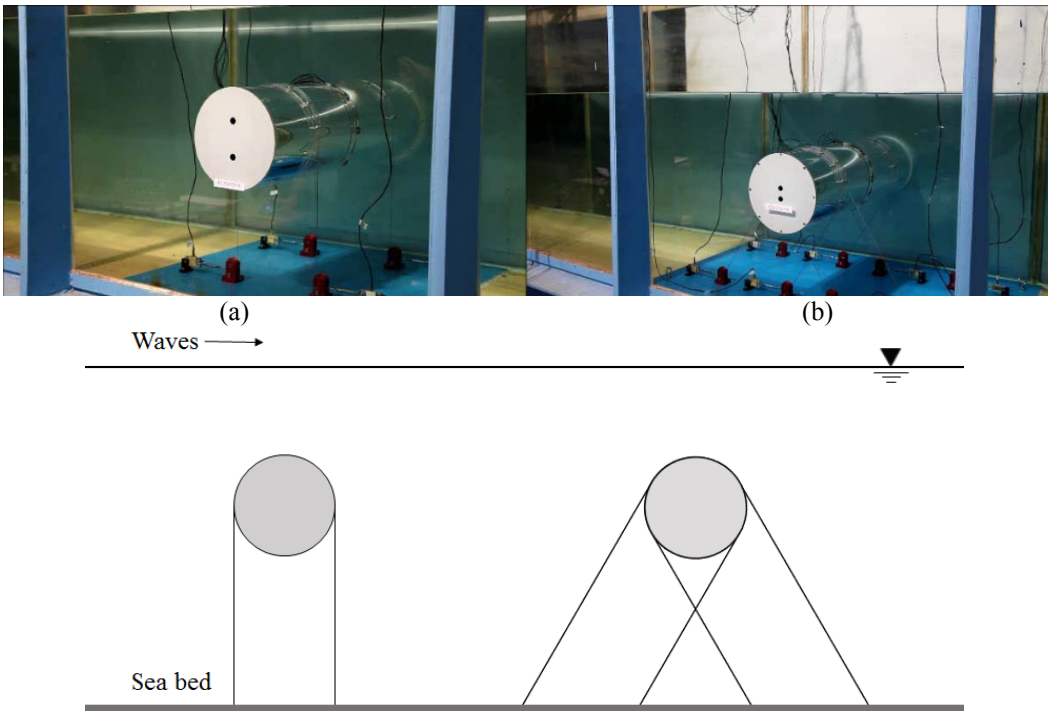

Fig. 2 Experimental configuration. (a) vertical mooring (VM) , (b)inclined mooring (IM)

Table 1 Experimental conditions

Parameter	Values
Diameter (m)	23
Water depth (m)	65 – 80 – 95
BWR VM	2.2 – 2.6 – 3.0
BWR IM	2.8 – 3.4 – 4.0
Wave period (seconds)	6.5 – 8.0 – 10.0 – 13.0
Wave steepness s	0.013 – 0.027 – 0.040 – 0.053

4. Results of coupled analysis

As presented in the previous section, the displacements of the SFT and forces on the tethers are the main focus of attention in this analysis. The variation of dynamic responses of the SFT under various wave conditions, water depth, and tether angles is investigated. In the case of CHARM3D, C_D is constant and equal to 1.2 while C_M is 2 considering a simple circular cylinder. In OrcaFlex, C_D is variable depending on flow conditions while C_M is equal to 2. On the other hand, the same

values are used for the calculation of hydrodynamic loads on tethers. In both codes, incident waves were modeled using Airy's linear wave theory.

For VM (vertical-mooring) configuration, the relationship between wave elevation, tunnel surge, and mooring tension is presented in Fig. 3. In this figure, the prototype condition is as follows: water depth is 80 m, wave period=13 s, wave steepness=0.04, and BWR=2.6.

From the figure, it can be observed that effective tension of the mooring lines and wave elevation are 180 degrees out of phase meaning that tension reaches its maximum value at wave trough. At this position, tethers are at vertical position since surge is zero. At the same time, the vertical acceleration of the SFT is at its maximum value pointing upwards. This combination generates the maximum tension on the tether. On the other hand, minimum tension is reached at the point where surge is maximum and vertical acceleration is minimum. At this point the SFT reaches its deepest position due to set-down effect, which is caused by an inverted-pendulum-like motion. We can also see some nonlinear behaviors of line tension.

The variation of heave and surge motions of the vertically moored SFT over the wave conditions tested, was calculated considering a particular water depth of 80 m and BWR equal to 2.6 for the vertically moored case. In Fig. 4, the results from experimental and numerical data are presented to validate the numerical-simulation schemes.

In the plots, the origin for surge and heave is located at the center of the tunnel. From the results of Fig. 4, numerical simulations agree well with experimental data. The trends in surge and heave motions are well captured validating the approach applied in both numerical schemes. Surge motion is directly related to wave height and wave period. For small and short waves, the response of the tunnel is small even considering the freedom of motion in this mode since the mooring lines do not restrict horizontal motion.

As waves increase in height and period, the surge becomes significant. The particle kinematics of longer waves penetrate deeper to more activate the SFT motions. Due to the vertical restriction by vertical mooring system, heave motion is insignificant for most of the wave conditions. Heave motion only becomes significant in the negative direction for large periods and high waves, which is caused by large surge through set-down effect.

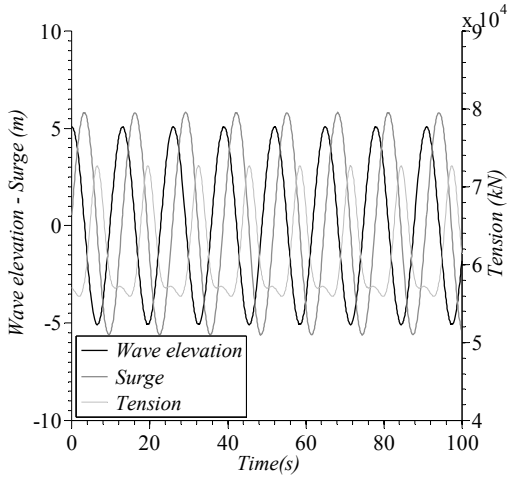

Fig. 3 Wave elevation, surge, and tension variation

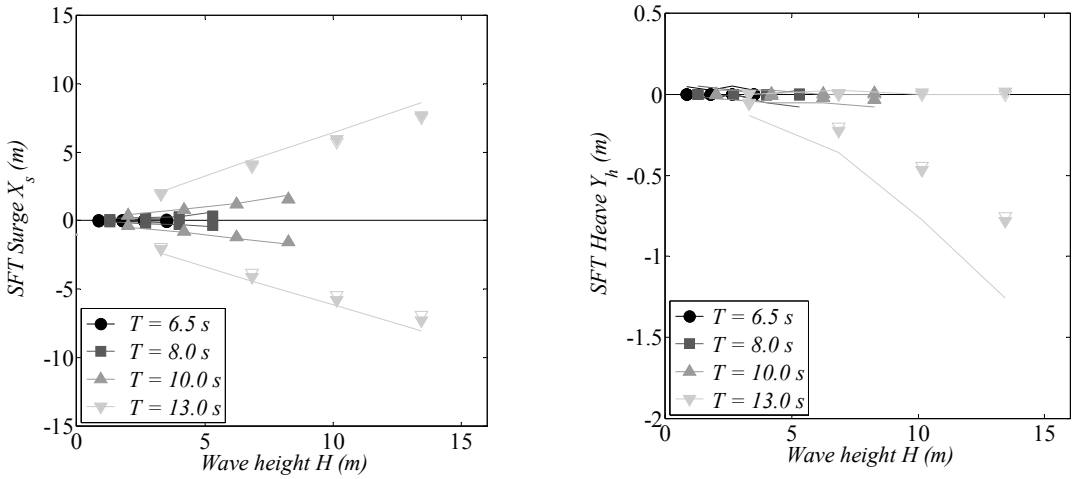

Fig. 4 (a) Surge and (b) Heave SFT displacements as function of wave height/period. (Solid lines=experiments, solid markers=CHARM3D results, and open markers=OrcaFlex results)

The correlation shows that both codes underestimate the negative maximum heave amplitude for the 13-s wave, which can be attributed to nonlinear effects associated with slack mooring, incident-wave deformation due to the presence of SFT, radiated waves caused by SFT motions, and typically large run wanted reflected waves for larger-period waves in experiments. Secondary viscous effects may not be important but may also contribute to the differences. The correlation between CHARM3D and OrcaFlex is also reflected in Fig. 4, where the results from both codes are close.

A particularly interesting condition to study is the 100 year return period storm defined by the Society of Submerged Floating Technology. This condition corresponds to a 13-s wave period and 0.04 wave steepness. The results for surge and heave under this particular condition as function of water depth and BWR are presented in Fig. 5 for the vertically moored SFT. The 65 m, 80 m, and 95 m water depths correspond to 15 m, 30 m, and 45 m submergence depth.

As BWR increases, so does the dynamic response of the tunnel both in surge and heave. This is due to the increase of surge stiffness so that its natural frequency is moving closer to the incident wave period as BWR increases. Both codes generate similar trend, which also agrees with experimental data. As intuitively expected, the dynamic responses of the SFT increase as submergence depths decrease. In the case of 13s wave period with wave steepness=0.04, the simulation results tend to underestimate the experimental values due to the reasons stated in regard to Fig. 4. For 80 m and 95 m water depths, wave field is minimally modified by the presence and motion of the structure, thus the numerical and experimental results tend to converge.

One important factor to consider when designing any floating offshore structure is the calculation of the maximum loading on station-keeping system. In this regard, mooring line tension as function of wave period and steepness is presented in Fig. 6. The case is for 80-m water depth and BWR=2.6. The plot represents the tension on a single mooring line since the signals from the four vertical mooring components are similar for any given wave condition.

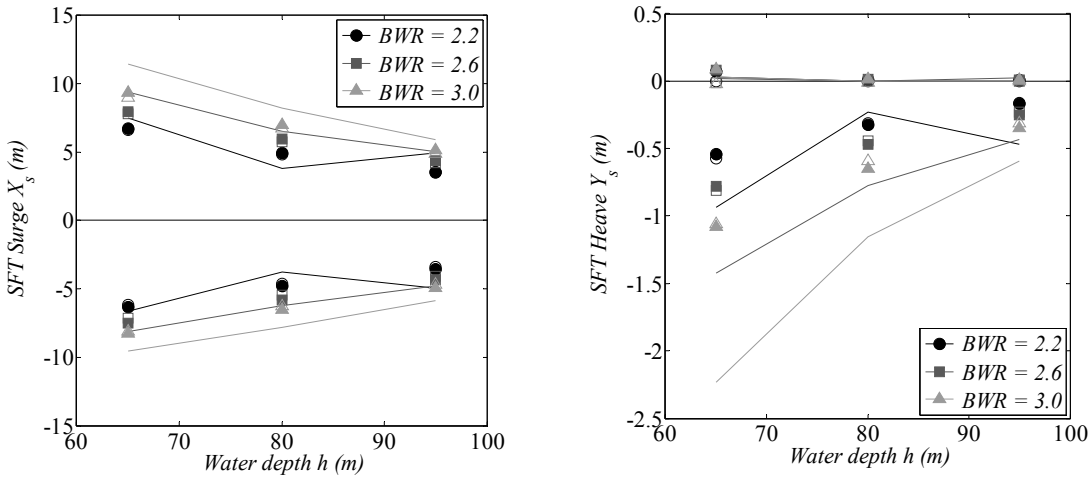

Fig. 5 (a) Surge and (b) Heave SFT displacements as function of water depth. Solid lines represent experiments, solid markers CHARM3D results and open markers OrcaFlex results

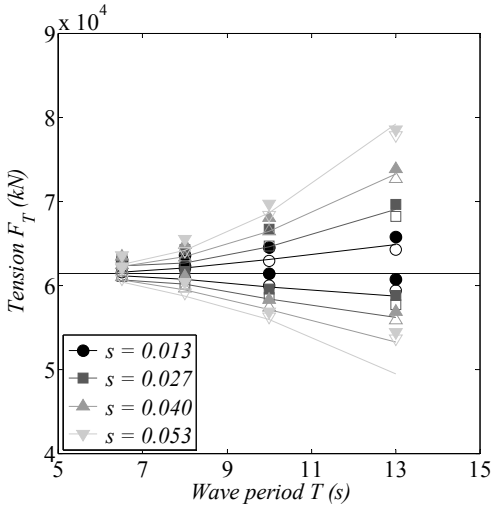

Fig. 6 Tension force on vertically moored SFT(Solid lines represent experiments, solid markers CHARM3D results and open markers OrcaFlex results)

Tension forces grow with wave period and wave height. Maximum and minimum loads are not symmetrical with respect to the initial pretension. This difference comes from nonlinear and set-down effects. The numerical simulations recover the general trends of experimental data. The small differences between CHARM3D and OrcaFlex results can be attributed to different methods in generating incident wave kinematics. In OrcaFlex, Wheeler stretching method was used instead of linear wave theory. As a result, we can observe the asymmetry on the vertical acceleration of

fluid at the given submergence depth, as shown in Fig. 7 for the 100-yr storm. The positive vertical acceleration is larger inducing a higher upward load. In the OrcaFlex case, it also needs to be reminded that variable drag coefficients are used for different flow conditions in calculating wave-induced drag forces.

The last set of data reveals the dynamic response of the submerged floating tunnel using the inclined mooring as shown in Fig. 2(b). This is an interesting alternative since the surge and heave responses are significantly reduced compared to the vertical-mooring case. In addition, the load is now distributed in 8 tethers. This configuration is intended to reduce the linear motions of the tunnel.

Unfortunately, no experimental data for surge and heave motions are available from the experimental paper. However, from the video recording, we can see that the motions are greatly reduced compared to the vertical mooring case, which can also be confirmed by the present numerical simulations, as shown in Fig. 8 (water depth=80 m, BWR=2.6). Even for high energy seas, the displacements of the structure are suppressed by the restriction of the inclined mooring (IM) system. It can be concluded that the inclined mooring system is very effective in minimizing SFT motions. Given the distribution of mooring lines being symmetric with respect to each other, the load is equally distributed and as in the case for vertically moored tunnel, the tension results for a single mooring line are also presented for the same case in Fig. 9. The effective tension on each line is reduced but the total mooring tension force increases when compared to the VM case since the displacements are much more restricted.

Finally, the experimental results for all wave periods for IM system are available for the case of 80-m water depth and BWR=3.4 and they are compared with OrcaFlex and CHARM3D numerical simulation results in Fig. 10. A similar trend as for the case of vertically moored tunnel is observed in this case. Mooring tensions increase as wave period and wave steepness increase. The rate of increase is almost linear with wave periods and heights. Both numerical simulations agree well with experimental data and present similar trends. Their differences are generally small. From the above comparisons, it is clear that the inclined-mooring-line arrangement presents better performance in terms of tunnel displacements and accelerations.

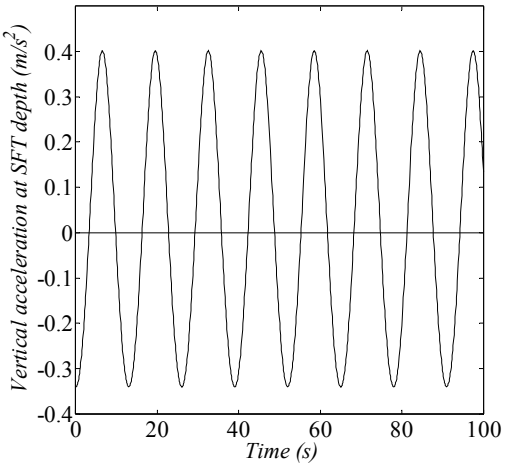

Fig. 7 Fluid acceleration by OrcaFlex at SFT depth

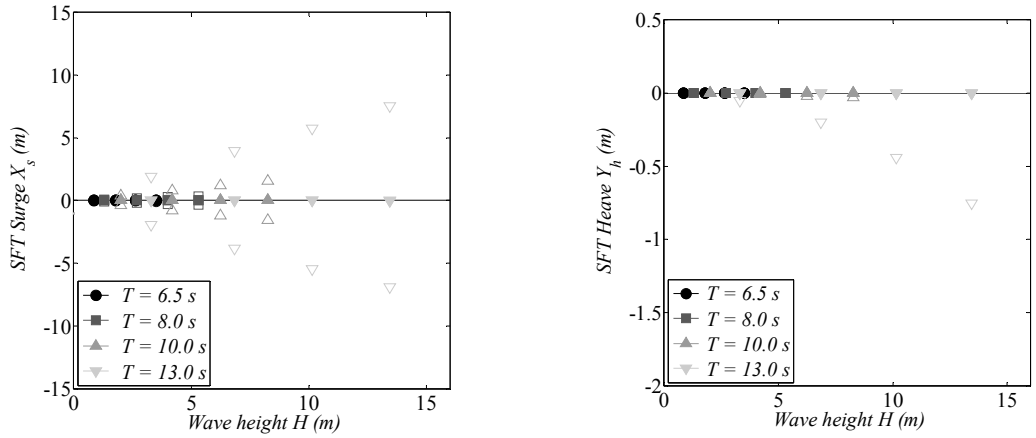

(a) (b)

Fig. 8 (a) Surge and (b) Heave SFT displacements for VM and IM as function of wave height and period(water depth=80 m, BWR=2.6; Open markers represent OrcaFlex results for VM configuration and solid markers OrcaFlex results for IM configuration)

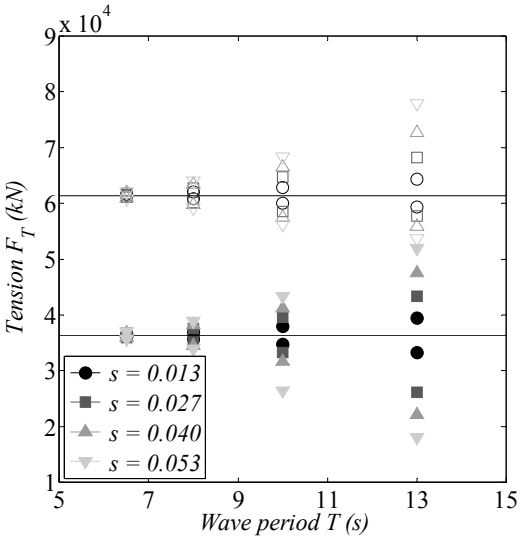

Fig. 9 Numerical results for Tension for VM and IM as function of wave height and period.(water depth=80 m, BWR=2.6; Open markers represent OrcaFlex results for VM configuration and solid markers OrcaFlex results for IM configuration)

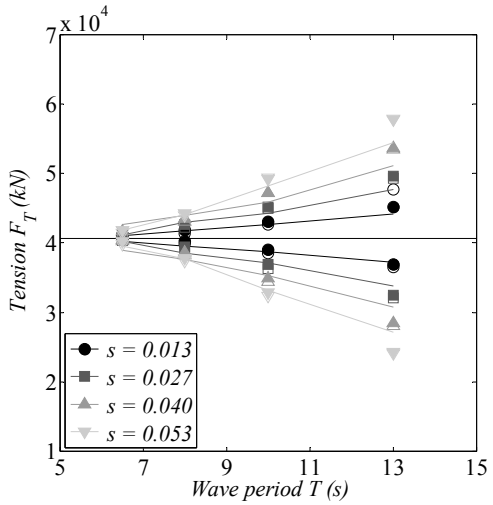

Fig. 10 Tension force oninclined mooring (water depth=80 m, BWR=3.4; Solid lines represent experiments, solid markers CHARM3D results and open markers OrcaFlex results)

5. Conclusions

The fully coupled dynamic analysis of a submerged floating tunnel under regular wave loading has been carried out. Main results obtained include translational (surge and heave) motions of the structure in addition to tension on the mooring system. Rotational motions are negligible for the given mooring system. The effect of several environmental factors were investigated including variation of water depth and wave conditions. The influence over the tunnel's responses due to structural parameters such as buoyancy to weight ratio and mooring line configuration was also included. Numerical results from two different software, OrcaFlex and CHARM3D, were compared against experimental data published by Oh *et al*. (2013) to validate the adopted approach. Overall, the numerical results show good agreement with measured data for a variety of wave conditions and structural parameters. Under high energy seas represented by long wave periods and large wave amplitudes, numerical results tend to deviate from experiments due to various nonlinear effects as discussed in previous sections.

Based on the obtained results, vertical mooring configuration presents a relatively large dynamic response especially for long wave periods. In this situation, the tunnel acts as an inverted pendulum causing set-down effects. If SFT is installed at deeper submergence depth, the dynamic response becomes smaller since wave action is reduced. At the same submergence depth, as BWR ratio increases so does the surge and heave of the structure. In terms of loading, for mild waves, the relation between wave period and force is almost linear while turning quadratic for high energy seas in case of vertically moored system.

In order to reduce the large translational response of the vertically moored configuration, an inclined mooring system, which can provide lateral stiffness to the SFT structure, was tested. Experimental and numerical results prove that the translational motions are significantly reduced for all the wave conditions considered under this mooring arrangement. In this case, tension at a single mooring line tends to follow a linear variation as wave period and height increase.

The variable C_D formulation depending on external flow conditions can improve the simulation

results especially for high energy waves, for which the velocity of the structure is significant, thus drag force plays more important role.

Overall, the submerged floating tunnel is a feasible concept and valuable information for the future development of this technology has been presented. Further analysis including hydro-elastic theory including fatigue, VIV in coexisting current, and snap loads in tethers is needed to provide a complete set of data for the successful design of a SFT structure.

Acknowledgments

The present study was financially supported by KIOST Korea.

References

Bae, Y.H. and Kim, M H. (2014), "Coupled dynamic analysis of multiple wind turbines on a large single floater", *Ocean Eng.*, **92**, 175-187.

Cifuentes, C. and. Kim, M.H. (2015), "Numerical simulation of wake effect in nets under steady current.", *Proceedings of the ASME 2015 34th International Conference on Ocean, Offshore and Arctic Engineering OMAE2015*.

DeCew, J., Tsukrov, I., Risso, A., Swift, M.R. and Celikkol, B. (2010), "Modeling of dynamic behavior of a single-point moored submersible fish cage under currents", *Aquac. Eng.*, **43**(2), 38-45.

Di Pilato, M., Perotti, F. and Fogazzi, P. (2008), "3D dynamic response of submerged floating tunnels under seismic and hydrodynamic excitation", *Eng. Struct.*, **30**(1), 268-281.

Eom, T.S., Kim, M.H., Bae, Y.H. and Cifuentes, C. (2014), "Local dynamic buckling of FPSO steel catenary riser by coupled time-domain simulations", *Ocean Syst. Eng.*, 4(3), 215-241.

Garrett, D.L. (1982), "Dynamic analysis of slender rods", *J. Energy Resour. Technol.*, **104**(4), 302.

Haritos, N. and He, D.T. (1992), "Modelling the response of cable elements in an ocean environment", *Finite Elem. Anal. Des.*, **11**, 19-32.

Hong, Y. andGe, F. (2010), "Dynamic response and structural integrity of submerged floating tunnel due to hydrodynamic load and accidental load", *Procedia Eng.*, **4**(1877), 35-50.

Jakobsen, B. (2010), "Design of the Submerged Floating Tunnel operating under various conditions", *Procedia Eng.*, **4**(1877), 71-79.

Kang, H. and Kim, M. H. (2014), "Hydroelastic analysis and statistical assessment of flexible offshore platforms", *Int. J. Offshore Polar Eng.*, 24(1), 35-44.

Kim, M.H., Koo, B.J., Mercier, R.M. and Ward, E.G. (2005), "Vessel/mooring/riser coupled dynamic analysis of a turret-moored FPSO compared with OTRC experiment", *Ocean Eng.*, 32(14-15), 1780-1802.

Kunisu, H., Mizuno, S., Mizuno, Y. and Saeki, H. (1994), "Study on submerged floating tunnel characteristics under the wave condition", *Proceedings of the 4th (1994) International Offshore and Polar Engineering Conference*.

Kunisu, H. (2010), "Evaluation of wave force acting on submerged floating tunnels", *Procedia Eng.*, **4**, 99-105.

Oh, S.H., Park, W.S., Jang, S.C., Kim, D.H. and Ahn, D.H. (2013), "Physical experiments on the hydrodynamic response of submerged floating tunnel against the wave action", *Proceedings of the 7th International Conference on Asian and Pacific Coasts (APAC 2013)*.

Orcina (2015), *OrcaFlex Manual Version 9.8a*. Ulverston, Orcina 2015.

Østlid, H. (2010), "When is SFT competitive?", *Procedia Eng.*, **4**(1877), 3-11.

Remseth, S., Leira, B.J., Okstad, K.M. and Mathisen, K.M. (1999), "Dynamic response and fluid / structure interaction of submerged floating tunnels", *Comput. Struct.*, **72**, 659-685.

Romolo, A., Malara, G. Barbaro,G. and Arena, F. (2008), "An analytical approach for the calculation of random wave forces on submerged tunnels", *Proceedings of the ASME 27th International Conference on Offshore and Arctic Engineering OMAE2008*.

Lu, W., Ge, F., Wang, L., Wu, X. and Hong, Y. (2011), "On the slack phenomena and snap force in tethers of submerged floating tunnels under wave conditions", *Mar. Struct.*, **24**(4), 358-376.

Lu, W., Ge, F., Wu, X. and Hong, Y. (2013), "Nonlinear dynamics of a submerged floating moored structure by incremental harmonic balance method with FFT", *Mar. Struct.*, **31**, 63-81.

Yang, C.K. (2009), *Numerical modeling of nonlinear coupling between lines/beams with multiple floating bodies*, Ph.D. Dissertation, Dept. Ocean Eng.,Texas A&M University.